Revived STIS: I.
Improved Calibration of the STIS Next Generation Spectral Library.

Don Lindler, *Sigma Space Corporation*
Sara Heap, *NASA/Goddard Space Flight Center.*

Abstract

The Space Telescope Imaging Spectrograph (STIS) Next Generation Spectral Library (NGSL) contains UV-optical spectra (0.2 to 1.0 microns) of 374 stars having a wide range in temperature, luminosity, and metallicity (http://archive.stsci.edu/prepds/stisngsl/). These spectra were obtained without centering the star in the 0.2 arcsecond slit. Mis-centering resulted in up to 10% errors in the calibrated flux. With the recent repair of STIS, we were able to obtain calibration data to characterize the wavelength-dependent throughput of the 0.2" slit versus the target's position within the slit. To apply this information, we first determined the amount by which each NGSL star is mis-centered using the location of fringes in the long wavelength (G750L) spectra (compared to the fringes in a reference tungsten flat). We were then able to derive the absolute flux distribution of each NGSL star.

Support for Program numbers HST-AR-11755 and HST-GO-11652 was provided by NASA through a grant from the Space Telescope Science Institute, which is operated by the Association of Universities for Research in Astronomy, Incorporated, under NASA contract NAS5-26555.

Reduction of the NGSL spectral

Improvements over the Standard ST ScI Pipeline Calibration

1. New spectral trace files were produced using the average spectral y-position versus x-position for the 52X0.2E1 aperture for all of the NGSL stars. CALSTIS adjust the trace by a constant offset for each individual observation.
2. Improved background subtraction. ST ScI pipeline uses only a lower background taken 300 pixels below the spectrum. We use both an upper and lower background taken much closer to the spectrum (30 pixels).
3. Larger extraction slit height (11 instead of 7) to improve overall photometric at the cost of some loss in S/N.
4. Custom wavelength dispersion coefficients created for the E1 aperture position.
5. Custom sensitivity curves were created for the 52X0.2E1 aperture using observations of BD+75D325 centered in the aperture.
6. Correction for mis-centering of the target within the slit using the G750L fringe flat to determine the target's position.
7. Zero-point wavelength correction using stellar lines. (no Wavecals were taken with the observations)

Measurement of the position of the target within the 52X0.2 aperture

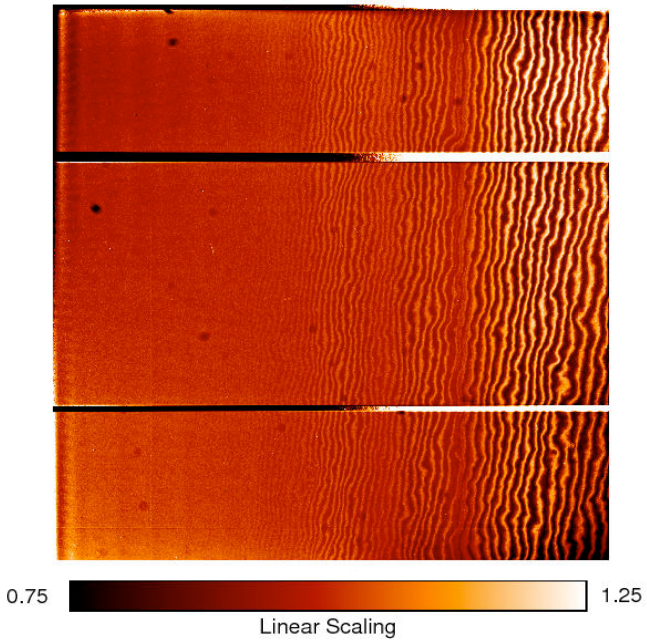

Fig. 1: Tungsten Lamp flat field taken in the 52X0.2 aperture with the G750L grating.

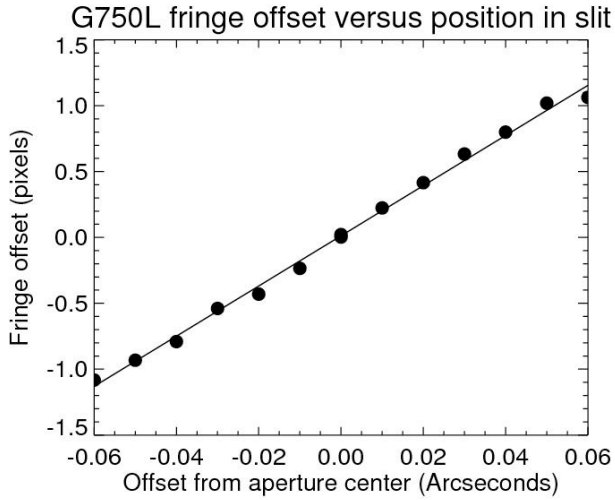

Fig. 2: Cross-correlation offset between fringes in the tungsten flat with the fringes in the stellar spectra vs offset of the target from the center of the slit.

Figure 2 illustrates that we can accurately measure the mis-centering of the target within the slit using the long wavelength fringes (Figure 1) in a tungsten lamp flat field exposure.

Correcting the Long Wavelength G750L Fringes

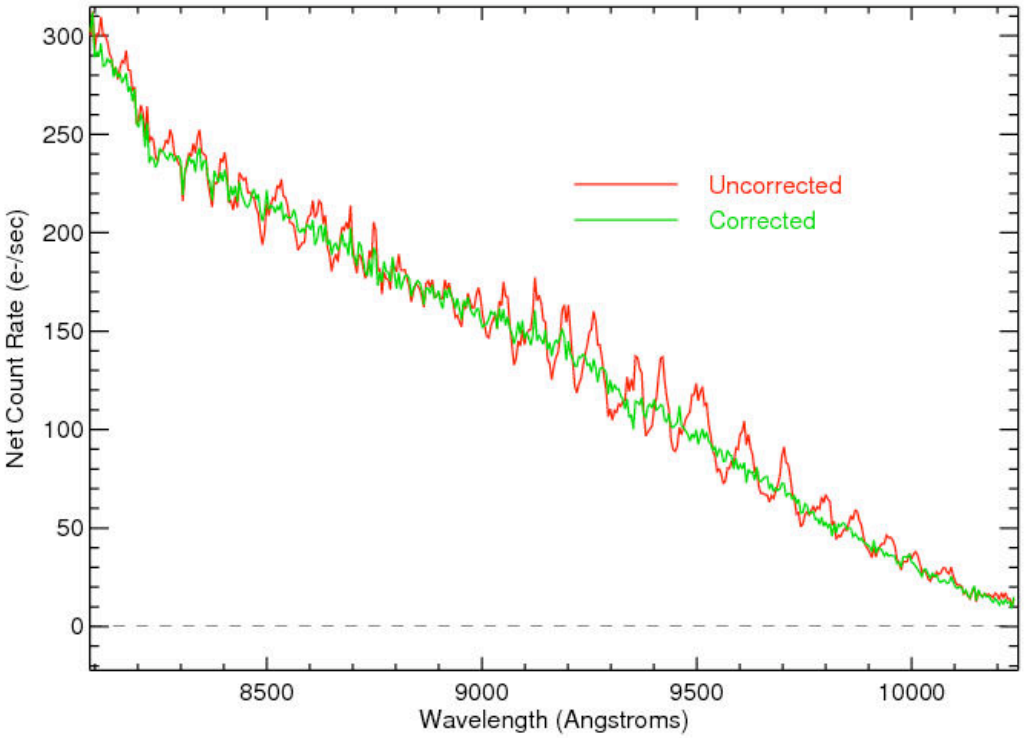

Fig. 3: Correction of the fringes in a stellar observation.

Once the offset of the fringes have been determined, the can be removed from the stellar spectrum (Figure 3).

Aperture Throughput Correction

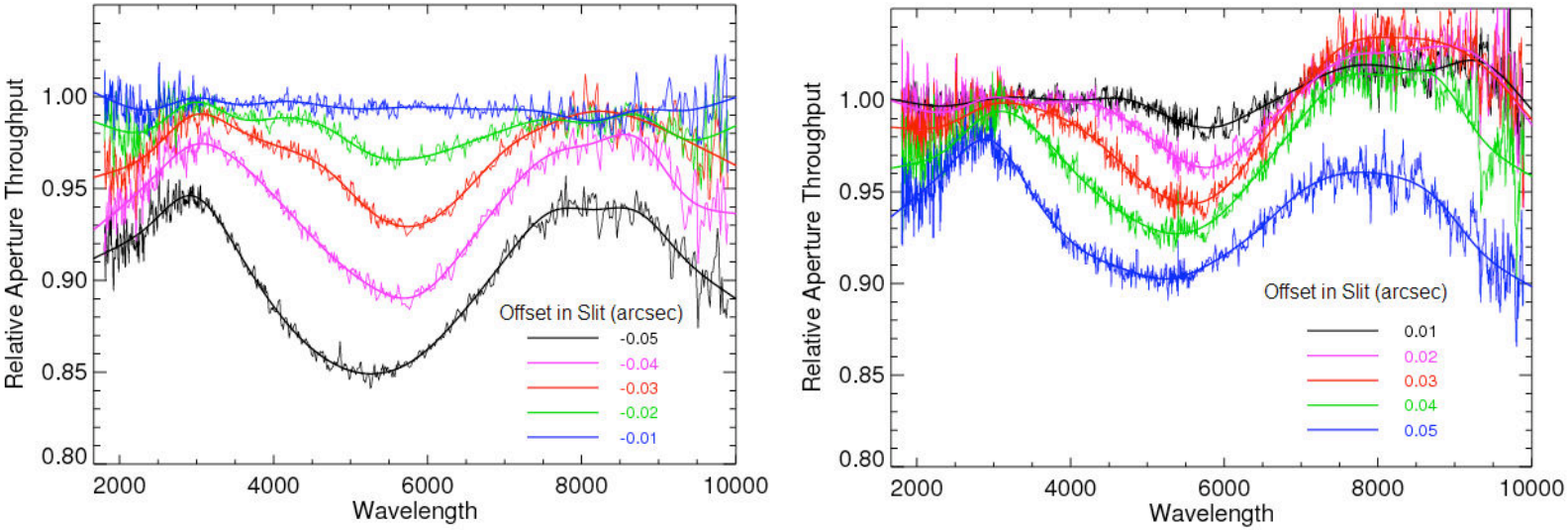

Fig. 4: Relative aperture throughput versus position of the target in the 52X0.2 slit

Figure 4 shows the relative throughput of the 52X0.2 aperture using calibration observations of BD+75D325 placed at different positions within the slit. Note that the point spread function is asymmetrical. Mis-centering in the +x direction can increase the throughput at the longer wavelengths.

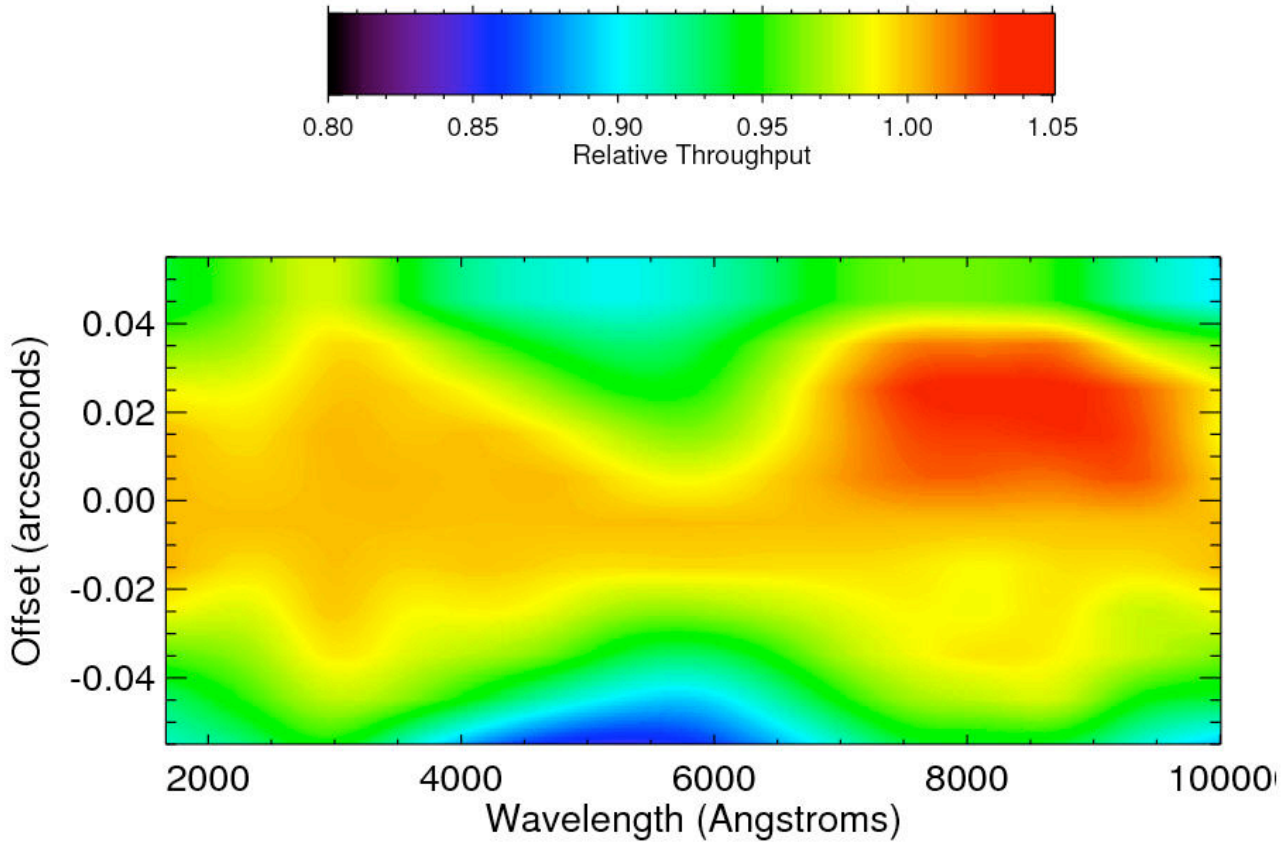

Fig. 5: Map of the relative aperture throughput of the 52X0.2 slit versus wavelength and offset from the center of the slit.

Wavelength Zero Points

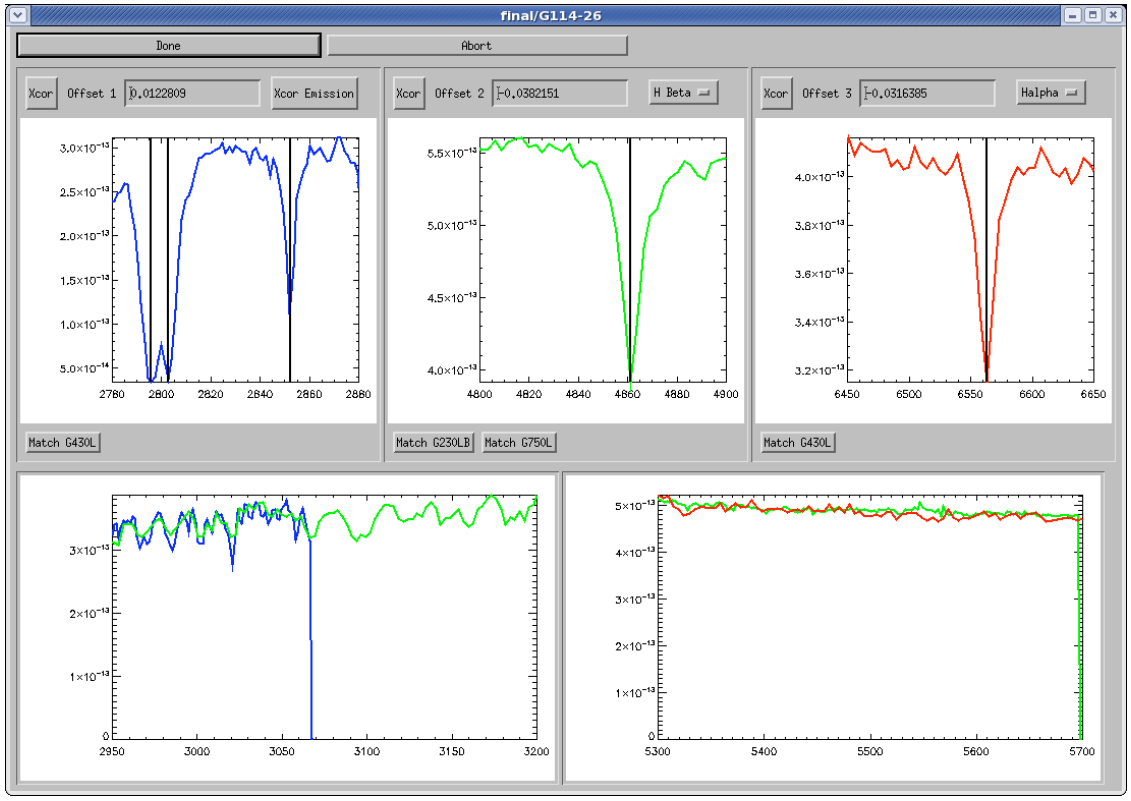

Fig. 6: Interactive tool for determining the Wavelength zero points.

The NGSL Spectra were taken without wavelength calibration lamp exposures. We use stellar features to determine the wavelength zero points for each of the three gratings. As a result, the final wavelength scales are in the rest frame of the star.

Correction of the G230LB in-order grating scatter

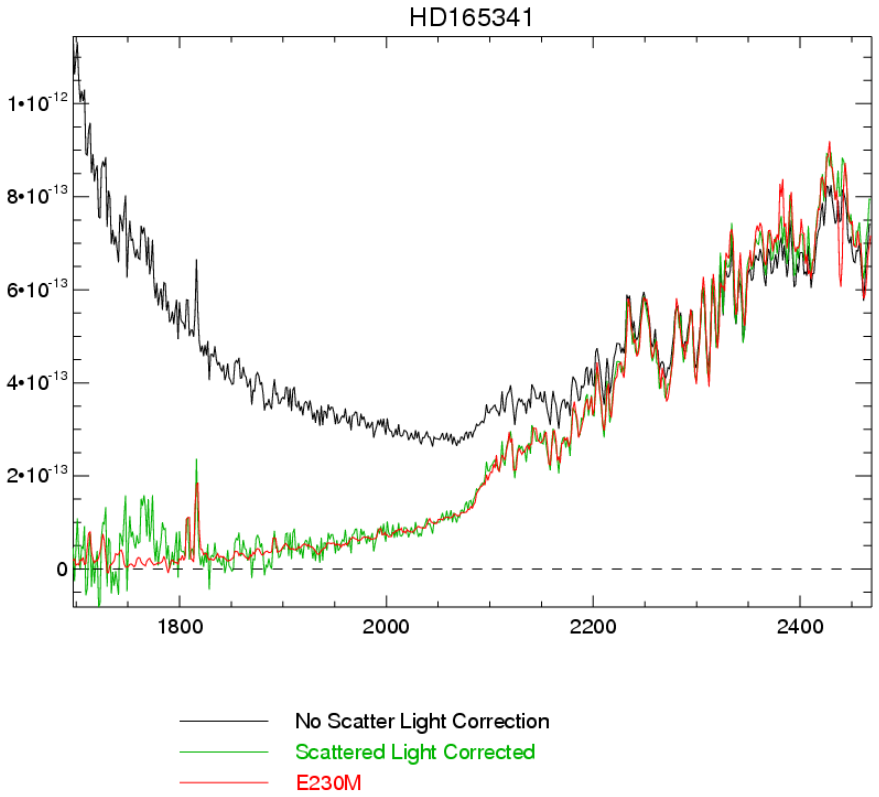

Scattered Light Model

Residual Net Rate = c0 (1+B*x)

Where:

x is the pixel number (0 to 1023)

$c0 = A \int C(\lambda) / \lambda^3$

(Integrated from 2,000 to 10, 000 Angstroms)

λ is the wavelength in Angstroms

$C(\lambda)$ is the net count rate/pixel
(computed using the observed flux with no scattered light correction and prelaunch component efficiencies)

A and B are computed from the 103 reddest stars in the library with almost no flux in the short wavelength end of G230LB.

A = 0.00246

B = 5582.5

Fig. 7: The G230LB has a significant in-order grating scatter. We have constructed a model to remove this scatter using the reddest stars. The figure shows that after correction the G230LB flux levels match an E230M observation.

The stellar parameters (L_{bol}, T_{eff}, ilog g, logZ, α, E(B-V)) are derived from NGSL spectra and distances via Castelli's (2004)/Marcs (2008) model spectra and the Basti evolutionary isochrones.

- Make χ^2 fit to spectrum ($\Delta\lambda$=0.20 -1.00 μ) for T_{eff}, logZ, and E(B-V)

- Determine L_v range corresponding to V, π, e_π

- Calculate L_{bol} from BC(T_{eff}, log Z, E(B-V))

- Determine range in distance (using new reduction of Hipparcos data, 2007, and a two sigma error for the parallax.

- Derive allowed range in ilogg via comparison with Basti evolutionary models

- Make χ^2 fit to spectrum for best ilog g